Cognitive Wireless Charger: Sensing-Based Real-Time Frequency Control For Near-Field Wireless Charging

Sang-Yoon Chang*† Sristi Lakshmi Sravana Kumar† Yih-Chun Hu†‡
*University of Colorado Colorado Springs, Colorado, USA
†Advanced Digital Sciences Center, Singapore
‡University of Illinois at Urbana-Champaign, Illinois, USA
schang2@uccs.edu, {sravana.s, yihchun}@adsc.com.sg

***Abstract*—A recent increase in mobile and IoT devices has led to the advancement of wireless charging. The state-of-the-art wireless charging systems operate at a particular frequency, controlled by the explicit networking from the power-receiving device (which relays the battery status information, useful for the frequency selection), but such control is not designed to cope with the variations in the power-receiving device's placements and alignments (which are more significant in near-field and pseudo-tightly coupled charging applications, as more charging pads are being deployed in the public domains and serving heterogeneous clients). In this work, we analyze the impact of the power transfer performance caused by the power receiver's load, distance, and coil alignment/overlap and introduce cognitive wireless charger (CWC), which adaptively controls the operating frequency in real-time using implicit feedback from sensing for optimal operations. In addition to the theoretical and LTSpice-based simulation analysis, we build a prototype compatible to the Qi standard and analyze the performance of CWC with it. Through our analyses, we establish that frequency control achieves performance gains in inductive-coupling charging applications and is sensitive to the variations in the placement and alignment between the power-transmitting and the power-receiving coils. Our prototype, when CWC is turned off, has comparable performance to the commercial-grade Qi wireless chargers and, with CWC enabled, demonstrates significant improvement over modern wireless chargers.**

I. Introduction

People's increasing reliance on mobile and embedded devices led to greater advancements in wireless power transfer. While wireless networking and mobile computing, respectively, focus on the connectivity and the operations of wireless devices, recent advances in power transfer envisions the wireless experience to extend to when the devices are getting charged, so that the customers can do so without the inconvenience of charging cables. In addition to personal charging pads (which is customized and tightly aligned to the customer's personal device receiving the power), public domains (such as restaurants, airports, and car traffic roads) are also deploying public charging pads so that the customers can charge their devices on the go; such public charging infrastructure introduces a necessity to embrace greater flexibility in devices placements, makes, and models.

In the evolving wireless charging landscape, we improve the power transfer by incorporating adaptive control on the power transmitter. We consider low-frequency inductive-coupling charging with battery-operated devices, as low-frequency inductive coupling has better power transfer performance than high-frequency or radio-frequency charging technology and is thus currently the most widely deployed power transfer technology, e.g., Qi technology governed by Wireless Power Consortium [1]. We further motivate our target systems to be low-resistance load applications, e.g., battery-operated systems, by deriving fundamental results about control sensitivity and how the performance gain can be more significant than in high-load or far-distance applications.

Our work is inspired by cognitive radio in wireless networking and software-defined radio tools that facilitates its implementation. *Cognitive radio* shares the network's spectrum resource by incorporating flexible and adaptive control in its communications parameter (e.g., center frequency and bandwidth) and is inherently required to avoid the primary user's operations *at all times* and *with no aid from the primary user*. The similarity between our work and cognitive radio goes beyond the apparent feature of incorporating adaptive parameter control. Like cognitive radio, our scheme is *constantly aware of the receiver statuses without using explicit feedback* and *controls the software-friendly frequency parameter*, making it very lightweight in hardware. Both features also distinguish our work from other previous work incorporating control in wireless charging (which we discuss in Section II); also, in contrast to prior work, we consider other factors affecting the power transfer (beyond the battery status and load resistance) when designing cognitive wireless charger. Due to similarity and the influence that cognitive radio had in our design, we call our scheme *cognitive wireless charger* (CWC).

CWC transmitter does not rely on the networking from the receiver but rather uses sensing (based on the signal measured across its *own* coils) for frequency control. CWC thus inherently bypasses the compatibility issues that can arise from having heterogeneous clients; for example, as of July 2016, there were more than 140 commercialized Qi-certified client devices in smartphones and tablets. Furthermore, CWC provides ef-

fective power transfer optimization even when the networking fails (our preliminary result shows that the demodulation in the networking practically becomes a coin flip when the distance to the client exceeds 2cm in a perfectly aligned and configured lab setting, which is unsurprising because the Qi receiver communication uses reflection-based backscattering, preserving energy but susceptible to channel noise); in fact, CWC works even when there is no/mismatched networking and can provide backward-compatibility to protocol-outdated clients as long as they are equipped with the capable hardware.

In addition to designing and building CWC, we share two important findings of inductive-coupling charging in this work. First, we study the feasibility of leveraging the coupled field to forgo explicit feedback from the receiver, whose performance we aim to maximize. Second, we analyze the impact of the load resistance and regulator implementation on frequency-based adaptive control, motivating our application scope to be aligned with the widely-used Qi standard (tightly coupled inductive coupling for battery-equipped clients). These findings have significant influence on our CWC design.

The rest of the paper is organized as follows. In Section II, we outline the application scope of our work and review relevant literature. Theoretical analyses and LTSpice-based simulations, forming the fundamental bases for our work, follow in Section III. We introduce CWC in Section IV and build our prototype in Section V-A. Afterward, we evaluate our prototype in Section V-B and conclude the paper in Section VI.

II. Our Application Scope & Related Work

Since the early 20th century, wireless power transfer is enabled between physically separate inductor coils using the electromagnetic (EM) field coupling [2]. Generating an alternating current (AC) in the transmitter's inductor coil produces a magnetic flux around the coil. When the receiver inductor coil is placed close to the transmitter coil, it consequently generates AC in the receiver circuit and the induced power can be used to power electronic components or charge the battery. A charging system can improve its performance by adding a capacitor to the inductor coils and tuning the system to operate at the resonance frequency [3], which value depends on the circuit design, e.g., the inductance and the capacitance of the system. CWC builds on such resonance technology.

We focus on tightly-coupled wireless charging systems and design our work to be compatible to the Qi standard [1], [4], the most widely adopted for mobile devices and operating in the 110-205 kHz frequency range and in the distance range in the order of centimeters. Tightly coupled wireless power transfer contrasts with loosely coupled in that it is designed for closer-distance applications and is significantly more efficient in power transfer. In addition, tightly coupled wireless power transfer has traditionally been used for applications where the transmitter's and the receiver's coils are perfectly aligned. Due to the rigid alignment between the coils, e.g., using physical magnets to aid alignment, there are very limited fluctuations across different charging sessions in the physical orientation of the receiver's coil with respect to the transmitter's; thus, in tightly coupled regions, receiver shares its load resistance or battery status to dynamically control the power transfer operations. Such tightly coupled model with limited factors for dynamic control is more suitable in the traditional wireless charging where the transmitter and the receiver are tightly paired and share the same manufacturer and model.

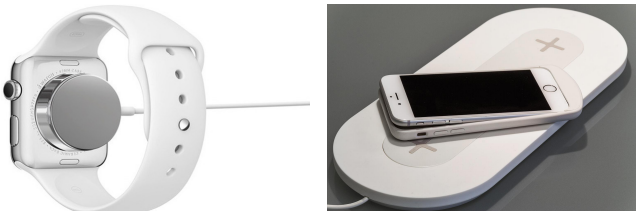

(a) Tightly coupled (b) Pseudo-tightly coupled

Fig. 1. Pictures depicting tightly coupled and *pseudo-tightly* coupled transfer

In the emerging charging landscape where the charging pads deployed in the public sector serve heterogeneous clients, there are greater variations in the transmitter-receiver charging dynamics, and we thus incorporate intelligence to conduct power transfer that is sensible to such fluctuations. As they are designed for near-distance wireless charging, we call them *pseduo-tightly coupled* regions and provide a representative example in Figure 1.[1] Pseudo-tightly coupled charging requires much less synchronization overhead (discovering the client is sufficient) than loosely coupled charging for longer-distance charging (for example, recent work supporting device mobility requires explicit handshaking and the client localization to start the power transfer [5], [6]). Like the power control networking for charging status sharing, our contribution is not to bootstrap the power transfer but to make the ongoing power transfer more efficient during the charging process.

Similarly to our work, previous researchers adopted adaptive frequency control to improve power transfer performance but for loosely coupled wireless power transfer applications [3], [7], [8] where such adaptive control is a direct byproduct of the information exchange from the explicit and inherently required synchronization and re-synchronization (e.g., client localization for mobile clients). In addition to targeting different applications than ours, these work have operating frequencies in the MHz range and introduce design issues such as conflicts with the ISM frequency band [8] and physiological challenges introduced to human bodies [9].

In near-field charging, others proposed to adaptively control the inductance and capacitance [7], [10], [11] or the receiver coil placement [12], [13], which consequently affect the power transfer characteristics such as the power/current amplitude. Such control requires modifications at the hardware level, which are more difficult and consumes more power than software-based modifications. CWC is orthogonal and can complement these approaches.

[1]Public charging pads sometimes deploy multiple coils interleaving their use depending on the receivers' number and positions. We focus on single transmitter coil and leave multiple-coil sensing and control for future work.

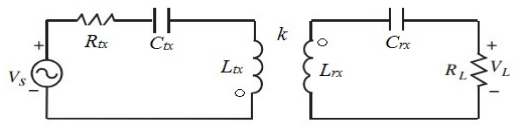

Fig. 2. Equivalent circuit representation for wireless charging

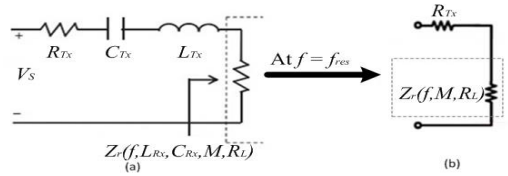

Fig. 3. (a) Equivalent circuit from the transmitter's view where Z_r is the reflected impedance due to the receiver (b) Equivalent circuit from the transmitter's view at $f = f_{res}$

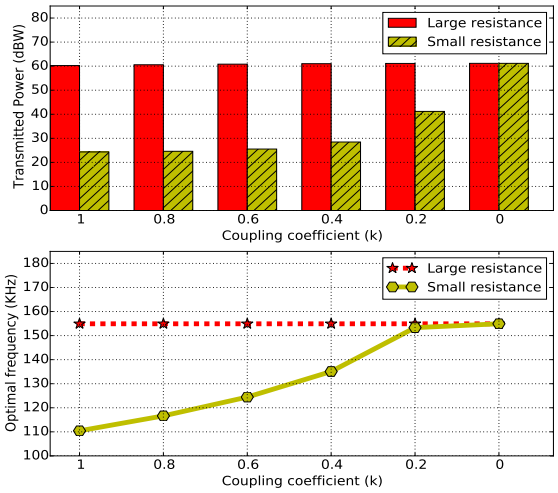

Fig. 4. The output power (top) and the optimal frequency (bottom) from the transmitter's perspective

III. Theoretical Analysis and Simulations

A. Theoretical Analysis on Reflected Impedance

Wireless charging system can be modeled by an equivalent circuit representation shown in Figure 2. To transfer power from the transmitter (left in Figure 2) to the receiver (right), the transmitter introduces an AC voltage source (V_S), and the variations in the electrical current generates inductive coupling on the receiver. For clarity, we define the following parameters:

- *Operating frequency* (f) is our control parameter and the frequency at which transmitter operates its AC current.
- *Resonant frequency* (f_{res}) is the frequency that results in the maximum power transfer in *loosely-coupled* inductive-coupling charging. It also corresponds to the maximum power sensed at the transmitter output in the absence of receiver but not in the pseudo-tightly and tightly coupled regions, as we will study in Section III-B and Section V-B.
- *Coupling coefficient* (k) is the ratio between the received signal amplitude (V_{rx}) and the transmitted signal amplitude (V_{tx}) and can take values between 0 and 1. k being equal to 0 corresponds to when the coils are not coupled, and k equal to 1 is when the coils are perfectly coupled.

In tightly-coupled inductive coupling, the receiver's presence affects the coupling field and thus the transmitter's electrical behavior. On the other hand, if the receiver is far away and the inductive coupling becomes loosely coupled, corresponding to $k \to 0$, then the transmitter's electrical behavior becomes oblivious to the receiver. To further explain this, we introduce the *reflected impedance* (Z_r) that is experienced by the transmitter due to the receiver's presence. Using Kirchoff's Voltage Law from Figure 2 yields:

$$Z_r = \frac{\omega^2 M^2}{Z_{rx}} = \frac{\omega^4 C_{rx}^2 M^2 R_L - j\omega^3 C_{rx} M^2 (\omega^2 C_{rx} L_{rx} - 1)}{(\omega^2 C_{rx} L_{rx} - 1)^2 + \omega^2 C_{rx}^2 R_L^2} \tag{1}$$

where ω is the angular frequency, i.e., $\omega = 2\pi f$, and M is the mutual impedance, i.e., M = $k\sqrt{L_{tx} L_{rx}}$.

At resonant frequency, i.e., $f = f_{res} = \frac{1}{2\pi\sqrt{L_{tx} C_{tx}}}$, the impedance across the receiver inductance (L_{rx}) gets cancelled by the impedance across the receiver capacitance (C_{rx}), and thus the reflected impedance does not depend on L_{rx} and C_{rx}, as depicted in Figure 3. If the inductance and capacitance of transmitter and receiver circuits are equal ($L_{tx} = L_{rx} = L$ and $C_{tx} = C_{rx} = C$), the reflected impedance becomes:

$$Z_r = \frac{\omega_{res}^2 k^2 L^2}{R_L} = \frac{4\pi^2 f_{res}^2 k^2 L^2}{R_L} \tag{2}$$

We omit further details and summarize our theoretical analysis in this section due to the space constraint; our impedance analysis agrees with prior literature [14]–[16]. In Section III-B, we study how the load resistance R_L affects Z_r, which heavily affects the power transfer, and how the optimal frequency is different from f_{res} in pseudo-tightly coupled charging regions.

B. Simulation Results

We design the wireless charging system using the circuit schematic in Figure 2 and choose the parameters to emulate our prototype design, described in Section V-A; the parameter values are $L_{tx} = L_{rx} = L = 24\mu H$, $C_{tx} = C_{rx} = C = 44nF$ and $R_{tx} = 1\Omega$. While the prototype evaluation in Section V-B focuses on CWC, we study the generic wireless charger behavior in this section.

According to Equation 2, Z_r depends on the f, k, and R_L, where f operates in 110-205 kHz according to the Qi standard and the FCC regulations on wireless charging. To further study the effect of k and R_L on Z_r and on the power transfer, we use LTSpice simulator (popularly used for hardware circuit schematic design) and vary k and f. We conduct our simulations with two different loads to contrast the behavior. First, we use a *large resistance* of $R_L = 10$ kΩ. For such large resistance, the overall impedance of the

transmitter (i.e., $Z_{tx} + Z_r$) remains relatively constant (with its magnitude varying between 1.03 Ω and 1.09 Ω with respect to k), and varying the coupling strength k does not make a significant impact on the charging behavior. Second, we use a *small resistance* of $R_L = 10$ Ω, in which case, the coupling strength makes a greater impact on the charging behavior; the magnitude of the transmitter impedance $Z_{tx} + Z_r$ varies between 1.03 Ω and 58.53 Ω for $0 \leq k \leq 1$. When $k = 0$ (loosely coupled), the receiver's presence and whether it has high-resistance load or low-resistance load does not affect the transmitter, i.e., $Z_r = 0$, and the magnitude of Z_{tx} is 1.03 Ω.

Figure 4 shows the effect of the impedance change on the transmitter power and the optimal frequency for power transfer. When the load has a large resistance, varying k does not have an impact. In contrast, for small load resistance, k affects Z_r and consequently the transmitter's power performance and the optimal frequency; the top plot in Figure 4 shows the power when the operating frequency is the optimal frequency (for any other choice of operating frequency, the performance decreases). We also observe that the optimal frequency converges to the resonant frequency ($f_{res} = \frac{1}{2\pi\sqrt{LC}} = 154$kHz) as $k \to 0$, which result agrees with prior work's frequency choice of resonance frequency in loosely-coupled inductive charging [3], [17]. The receiver power monotonically increases with the transmitter power and thus, fixing the rest of the parameters (e.g., k), optimizing the transmitted power corresponds to optimizing the power transfer of the system; Section V-A studies the power transfer in the receiver's perspective.

Tightly-coupled inductive coupling introduces the coupling coefficient k to characterize how tight the coupling is between the transmitter and the receiver (loosely coupled region does not require such parameter as $k \to 0$). In this section, we establish that the load resistance magnitude plays a factor in determining the relevance of k in power transfer; if the load resistance dominates the reflected impedance, then k has very small impact on the power transfer. Since CWC's adaptive control is more relevant and can achieve greater gain when the power transfer is sensitive to k, the rest of our work operates not only in the pseudo-tightly coupled scenario (as described in Section II) but also when the load resistance is low, for example, low-power systems and battery-equipped systems.

IV. Cognitive Wireless Charger

As discussed in Section I, cognitive wireless charger (CWC) adapts its parameters to optimize power transfer. In contrast to other prior work that changes the power transmitter's hardware configurations [7], [10]–[13], we focus on the software-defined parameter for maximizing the power transfer; implementing control at the software level enables greater programmability/flexibility and provides finer granularity for adapting to varying placements and heterogeneous clients.

We specifically adapt the frequency parameter of the AC current. While our goal is to maximize the received power from the power receiver to expedite the charging process, CWC finds the frequency that maximizes the *transmitted* power measured from the transmitter side. To learn about the receiver's perspective, prior work uses networking and the receiver explicitly relaying its power transfer status to the transmitter, but such networking procedure is unnecessary because the wireless charging operates under the tightly coupled region; the transmitter can sense its own voltage and infer the voltage/power performance of the receiver because the transmitter's and the receiver's electromagnetic/electrical fields are tightly coupled and highly correlated. CWC's use of sensing (with no explicit networking) for power transfer optimization is novel to the best of our knowledge, and we verify its effectiveness in Section V-B.

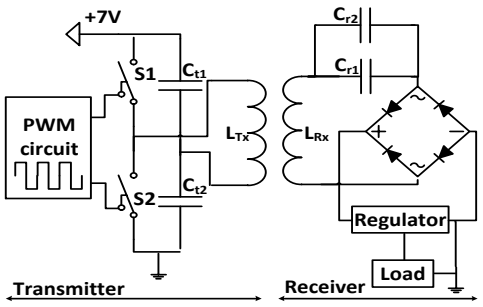

Fig. 5. Prototype implementation of wireless charger

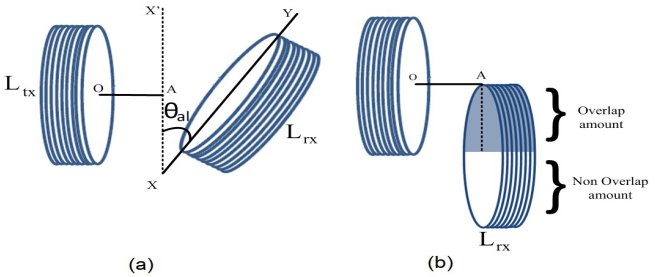

Fig. 6. Coil misalignment metrics: (a) Alignment angle and (b) Overlap

CWC is automatic and controls the frequency of the AC power via sensing-based learning in real time and can be useful to adapt to the receiver's dynamic battery status. The sensed voltage, measured across the transmitter's coil, drives a voltage-controlled oscillator (VCO) implemented inside the micro-controller, which in turn generates the AC voltage. CWC initially decreases the frequency from the resonant frequency (the optimal frequency when coupling coefficient approaches zero, as shown in Figure 4) and the sensed voltage acts as a negative feedback to the frequency control, i.e., further decrease the frequency if the voltage increases and increase the frequency if the voltage decreases. Such control is pervasively used in computing, e.g., phase-locked loop (PLL) for frequency tracking in wireless networking and for intra-host (one entity) battery charging control [18], and the optimization of such control (e.g., the convergence speed and the tradeoff between the optimality precision and the stability) is well-studied and beyond the scope of our contribution.

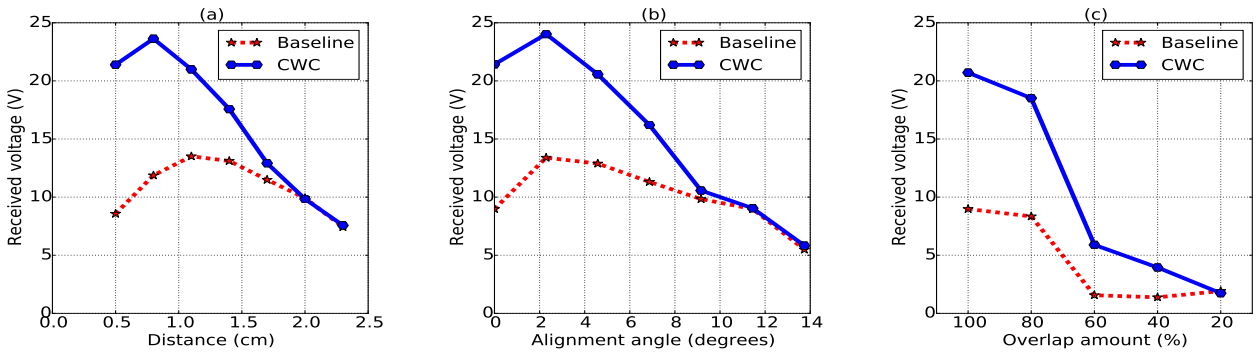

Fig. 7. CWC and the baseline performances for coil misalignments

V. Prototype Evaluation

A. Prototype Implementation

We design our prototype so that it is compatible to Qi standard [1] and describe it in Figure 5. We match the circuit impedance between the transmitter and the receiver and therefore, they have the same inductance/capacitance values; the inductance of the coils L_{tx} and L_{rx} are $24\mu H$, and equivalent capacitance of the capacitance combinations on both sides are $44nF$; the resonance frequency is $f_{res} = \frac{1}{2\pi\sqrt{LC}} = 154$kHz.

a) Transmitter: The transmitter circuit, described in figure 5 (left side), comprises of a pulse-width modulation (PWM) circuit and a switching circuit connected to the LC circuit of the transmitter. A STM32F4 Discovery Board generates a PWM signal to generate the AC current; the PWM frequency corresponds to that of the AC current. The PWM output is fed to TPS28225D driver to toggle the switches. When the PWM pulse is high, the upper switch S1 is turned on and the current flows through the upper switch and charges the inductor coil L_{tx} and capacitor C_{t2}. When the PWM pulse is low, the lower switch is turned on and upper switch off, and the stored current/voltage in the coil and capacitor C_{t1} is discharged through the lower transistor. Due to continuous toggling of the switches, AC voltage and current is generated across the inductor coil. With no receiver, the voltage and current is maximum when operating at resonant frequency.

b) Receiver: The receiver schematic, shown on the right side of figure 5, consists of an LC tank circuit, rectifier, and regulator. A Bridge rectifier is used in order to have a continuous DC output during both positive and negative half cycles. A linear voltage regulator, with a dynamic range (possible input voltage) of 7-30 V and an output voltage of 5V, is used to regulate the voltage delivered to the load; a voltage regulator is popularly used in wireless charging to provide stable power supply to the load; we study the effect of such regulator in Section V-B.

c) Backend processor: CWC algorithm is implemented in the computer connected to the transmitter microcontroller.

B. Experimental Results

1) Coil Misalignment Analyses: We conduct experiments to measure the CWC's steady-state performance and compare it with a *Baseline performance* when using the resonance frequency (which is only optimal when $k \to 0$ and is oblivious to the transmitter-receiver alignment). Also, we measure k as the voltage ratio between the received signal (V_{rx}) and the transmitted signal (V_{tx}). We first study the effect of the misalignment in distance and the orientation/angle between the transmitter coil and the receiver coil without the regulator (to better capture the physical phenomenon with the inductive coupling and separate the analyses with the particular regulator implementation) and then attach the regulator to study the effect of the regulator on adaptive control in Section V-B2.

In pseudo-tightly coupled charging, the coil placements and orientations are imperfect and the variations can have a significant impact on the coupling field and its strength k, which yields opportunities for frequency control for improving power transfer as we discussed in Section III-B. We study such variations here and specifically study the misalignment in distance, alignment angle, and the overlap amount between the coils; these misalignment metrics can vary because of the physical build of the transmitter and the receiver (e.g., the thickness of the mobile phone exterior/case) and their relative placements. For clarity, Figure 6 describes the metrics of alignment angle and the overlap amount in diagrams. Figure 7 shows the performances of CWC and the Baseline (fixing the operating frequency at f_{res}) with respect to the distance, alignment angle, and the overlap amount. Figure 7(b) and Figure 7(c) results are measured when the distance is 0.5cm (the typical distance arrangement for tightly-coupled Qi charging systems). As the misalignment in distance, alignment angle, and overlap amount, respectively, increases, the coupling strength consequentially decreases and the gains of using CWC over the Baseline also decreases; we observe the maximum gain of approximately 1.63x when the coils are best aligned, and the gain decreases as misalignment becomes greater, eventually converging to the Baseline, which is also the optimal operating frequency in a loosely-coupled region.

2) CWC on Regulator Design: In contrast to Section V-B1, we now study the system performance with the regulator. Regulator at the receiver increases the robustness in power

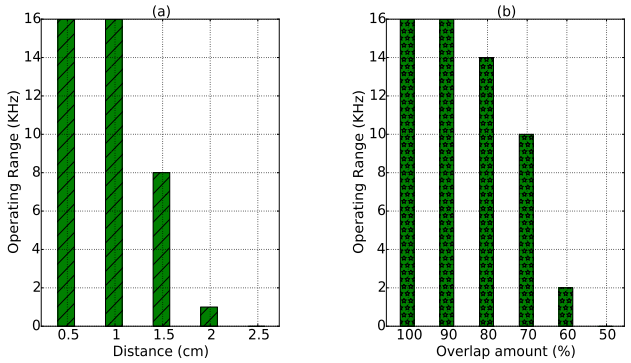

Fig. 8. System operating range with respect to coil misalignment

delivery by providing constant and stable power supply to the receiver load but loses power in the process, e.g., our linear regulator is designed to have a dynamic range of 7V-30V and output voltage of 5V (4.8-5.1V). In this section, we study how CWC can help the received voltage stay within the regulator's dynamic range (which defines the input voltages that enable the regulator's operation); if the input is not within the regulator's dynamic range, then the regulator shuts off and there is no power delivery. First, we investigate the receiver's coil misalignment sensitivity with the regulator (Section V-B1 studied the sensitivity without the regulator and the voltage performance in that section corresponds to the input to the regulator). Due to the long dynamic range (7V-30V) of our regulator implementation, the Baseline performance becomes more comparable to CWC's than the results without the regulator in Section V-B1. However, CWC still achieved power transfer gain over the Baseline in the pseudo-tightly coupled regions when there is a mismatch in the ovelap amount, which results are omitted due to space constraints.

We also study the frequency range that enables the regulator to operate and define the *operating range* to be the size of the operating frequencies providing power within the regulator's dynamic range. Unsurprisingly, as the coils become increasingly misaligned, the operating range decreases, providing greater constraints on the condition for the power-transfer system and less flexibility for frequency control; this behavior is shown when varying the overlap amount (Figure 8(a)) and the distance (Figure 8(b)). Therefore, CWC can aid in the regulator design by introducing looser/easier constraints on the dynamic range (and potentially increasing the output power).

VI. Conclusion

Cognitive wireless charger (CWC) uses sensing, rather than explicit networking, to adapt the charging system's operating frequency for greater power transfer efficiency. Effective in the pseudo-tightly coupled wireless charging applications (motivated by the increasing number of charging pads being deployed in the public domains and serving diverse mobile clients), CWC embraces the variations in the clients' builds and placements and offers significant power delivery gains.

Acknowledgment

This study is supported by the research grant for the Human-Centered Cyber-physical Systems Programme at the Advanced Digital Sciences Center from Agency for Science, Technology and Research (A*STAR), Singapore.

References

[1] Wireless Power Consortium, *The Qi Wireless Power Transfer System Power Class 0 Specification, Parts 1 and 2: Interface Definitions version 1.2.2*, April 2016.

[2] N. Tesla, "Apparatus for transmitting electrical energy." Dec. 1 1914, US Patent 1,119,732. [Online]. Available: http://www.google.com/patents/US1119732

[3] A. Kurs, A. Karalis, R. Moffatt, J. D. Joannopoulos, P. Fisher, and M. Soljacic, "Wireless power transfer via strongly coupled magnetic resonances," *Science*, vol. 317, no. 5834, pp. 83–86, July 2007. [Online]. Available: http://dx.doi.org/10.1126/science.1143254

[4] D. Van Wageningen and T. Staring, "The qi wireless power standard," in *IEEE Power Electronics and Motion Control Conference (EPE/PEMC)*, Sept 2010, pp. S15–25–S15–32.

[5] J. Jadidian and D. Katabi, "Magnetic mimo: How to charge your phone in your pocket," in *Proceedings of the 20th Annual International Conference on Mobile Computing and Networking (MobiCom)*. New York, NY, USA: ACM, 2014, pp. 495–506. [Online]. Available: http://doi.acm.org/10.1145/2639108.2639130

[6] B. Waters, B. Mahoney, V. Ranganathan, and J. Smith, "Power delivery and leakage field control using an adaptive phased array wireless power system," *Power Electronics, IEEE Transactions on*, vol. 30, no. 11, pp. 6298–6309, Nov 2015.

[7] B. Waters, A. Sample, and J. Smith, "Adaptive impedance matching for magnetically coupled resonators," in *Progress in Electromagnetics Research Symposium*, 2012, pp. 694–701.

[8] S. L. B.-J. Jang and H. Yoon, "Hf-band wireless power transfer system: concept, issues, and design," in *Progress In Electromagnetics Research*, 2012, pp. 211–231.

[9] J. Nadakuduti, L. Lu, and P. Guckian, "Operating frequency selection for loosely coupled wireless power transfer systems with respect to rf emissions and rf exposure requirements," in *Wireless Power Transfer (WPT), 2013 IEEE*, May 2013, pp. 234–237.

[10] S. O'Driscoll, A. S. Y. Poon, and T. H. Meng, "A mm-sized implantable power receiver with adaptive link compensation," in *IEEE International Solid-State Circuits Conference - Digest of Technical Papers*, Feb 2009, pp. 294–295.

[11] P. Si, A. P. Hu, S. Malpas, and D. Budgett, "A frequency control method for regulating wireless power to implantable devices," *IEEE Transactions on Biomedical Circuits and Systems*, vol. 2, no. 1, pp. 22–29, March 2008.

[12] D. Baarman, S. McPhilliamy, and C. Houghton, "Inductively powered apparatus," Oct. 10 2006, US Patent 7,118,240. [Online]. Available: https://www.google.com/patents/US7118240

[13] K. Lee, Y. Kim, K. Byun, and S. YEO, "Method for controlling charging power and wireless charging apparatus for the same," Jun. 2 2015, US Patent 9,048,683. [Online]. Available: https://www.google.com/patents/US9048683

[14] X. Liu, W. M. Ng, C. K. Lee, and S. Y. Hui, "Optimal operation of contactless transformers with resonance in secondary circuits," in *IEEE Applied Power Electronics Conference and Exposition (APEC)*, Feb 2008, pp. 645–650.

[15] ——, "Optimal operation of contactless transformers with resonance in secondary circuits," in *IEEE Applied Power Electronics Conference and Exposition (APEC)*, Feb 2008, pp. 645–650.

[16] H. S. Kim, D. H. Won, and B. J. Jang, "Simple design method of wireless power transfer system using 13.56mhz loop antennas," in *IEEE International Symposium on Industrial Electronics*, July 2010, pp. 1058–1063.

[17] R. Hui, "Rechargeable battery circuit and structure for compatibility with a planar inductive charging platform," Feb. 24 2009, US Patent 7,495,414. [Online]. Available: http://www.google.com/patents/US7495414

[18] L.-R. Chen, "Pll-based battery charge circuit topology," *IEEE Transactions on Industrial Electronics*, vol. 51, no. 6, pp. 1344–1346, Dec 2004.